NACA TN 3169

NATIONAL ADVISORY COMMITTEE
FOR AERONAUTICS

JUL 12 1954

TECHNICAL NOTE 3169

ON THE DRAG AND SHEDDING FREQUENCY OF

TWO-DIMENSIONAL BLUFF BODIES

By Anatol Roshko

California Institute of Technology

NACA

Washington

July 1954

NATIONAL ADVISORY COMMITTEE FOR AERONAUTICS

TECHNICAL NOTE 3169

ON THE DRAG AND SHEDDING FREQUENCY OF

TWO-DIMENSIONAL BLUFF BODIES

By Anatol Roshko

SUMMARY

A semiempirical study is made of the bluff-body problem.

Some experiments with interference elements in the wake close
behind a cylinder demonstrate the need for considering that region in
any complete theory.

Dimensional analysis of a simple model of the region leads to a
universal Strouhal number S^* which is then experimentally determined
as a function of wake Reynolds number R^*. This result, together with
free-streamline theory, allows the drag to be calculated from a measure-
ment of the shedding frequency and furnishes a useful correlation
between different bluff cylinders.

By allowing for some annihilation of the vorticity in the free
shear layers, it is shown how to combine the free-streamline theory
with Kármán's theory of the vortex street to obtain a solution
dependent on only one experimental measurement.

INTRODUCTION

The problem of the drag of bluff bodies in incompressible flow is
one of the oldest in fluid mechanics, but it remains one of the most
important, for practical reasons as well as for its theoretical interest

The two major contributions toward a theoretical understanding are
the well-known ones of Kirchhoff and Kármán. These attack two aspects
of the problem that must be understood, namely, the potential flow in
the vicinity of the cylinder and the wake farther downstream, but
neither by itself can furnish a complete theory. Much of the work
devoted to the problem through the years has been essentially the
elaboration and application of the theories of Kirchhoff and Kármán.

It has become increasingly evident, however, that a complete solution will not be obtained until one is able to "join" the two parts of the problem and that this will require an understanding of the flow in the early stages of the wake, that is, the first few diameters downstream of the cylinder.

On the experimental side, there has also been a continued activity. It is surprising that the influence on theoretical developments has been rather small, for considerable useful information has been compiled, some as long ago as 20 or 30 years. Much of this is referred to in chapters IX and XIII of reference 1. Particular mention must be made of the work of Fage and his coworkers (e.g., refs. 2, 3, and 4) who made very useful investigations of the flow near the cylinder and in the early stages of the wake. The ideas of this report grew largely out of a study of their work.

The interest at GALCIT in the flow past bluff bodies has been connected not so much with the problem of the drag as with that of turbulent wakes. Many of the turbulent flows that are used for experimental studies (e.g., behind grids) and almost all those that cause practical difficulties (e.g., buffeting) are produced in the wakes of bluff bodies. Much of the empiricism connected with these problems can be resolved only by a better understanding of how the wake is related to the body which produces it. This includes questions of wake scale, frequencies, energy, interference between wakes, and so forth. However, whatever the approach, one is led to consider the relation between the wake and the potential flow outside the wake and cylinder.

A short review of the theory of flow past bluff bodies is presented and some experiments are described which demonstrate how critically the whole problem depends on that part of the wake immediately behind the cylinder. In the remainder of the report the free-streamline theory of reference 5 is combined with some experimental results to obtain a much needed correlation between bluff cylinders[1] of different shapes. This furnishes at the same time some of the sought-after relations between wake and cylinder.

The experiments were performed in the 20- by 20-inch low-turbulence wind tunnel at GALCIT, under the sponsorship and with the financial assistance of the National Advisory Committee for Aeronautics. Standard

---

[1]The term "cylinder" is used throughout to denote a body whose cross-sectional shape is the same at every section along the span. This is the so-called two-dimensional body, which was the only kind for which measurements were made here. The term is applied to all cross-sectional shapes, including the limiting case of a flat plate normal to the flow, in which case the cross-sectional shape is simply a line.

hot-wire equipment, manometry, and so forth were employed. The work is part of a broader program of turbulence research directed by Dr. H. W. Liepmann; the author is indebted to him and to other members of the GALCIT staff for many discussions.

SYMBOLS

b' distance between outer edges of free shear layers

C_D drag coefficient

C_p pressure coefficient

C_{ps} base-pressure coefficient

c distance from back of cylinder to trailing edge of interference element

d cylinder diameter or breadth

d' distance between free streamlines

h width of vortex street

k base-pressure parameter, U_s/U_∞ or $\sqrt{1 - C_{ps}}$

k_T base-pressure parameter, uncorrected for tunnel blockage

l longitudinal vortex spacing

n vortex shedding frequency

p_s base pressure

R Reynolds number based on cylinder diameter, $U_\infty d/\nu$

R_T Reynolds number uncorrected for tunnel blockage

R^* Reynolds number based on wake parameters, $U_s d'/\nu$

S cylinder Strouhal number, nd/U_∞

S_T Strouhal number uncorrected for tunnel blockage

S^* wake Strouhal number, nd'/U_s

S' Fage's form of Strouhal number, nb'/U_∞

U velocity along shear layer

U_1, U_2 velocities at edges of shear layer

U_∞ free-stream velocity

$\Delta U_\infty/U_\infty$ blockage correction to measured free-stream velocity

U_S velocity on free streamline at separation

u velocity of vortices relative to free-stream velocity

x distance downstream

β angle measured from stagnation point of circular cylinder

Γ circulation per vortex

ϵ fraction of shear-layer vorticity that goes into individual
           vortices

ζ vorticity

η coordinate normal to shear layer

ν kinematic viscosity

REVIEW OF THEORY OF FLOW PAST BLUFF BODIES

        Although the main contributions to the theory of flow past bluff
bodies are well-known, a review is useful to bring out the important
features of the problem.

        In the free-streamline theory developed by Kirchhoff, the free
shear layers which are known to separate from bluff bodies are idealized
by surfaces (streamlines) of velocity discontinuity. These free stream-
lines divide the flow into a wake and an outer potential field. The
possibility of treating the problem this way in two parts is important
to note. Kirchhoff's theory, however, considerably underestimates the
drag, and the failure is easily traced to the assumption which is made
about the velocity on the free streamline. It is assumed that the
velocity there is the free-stream velocity or, what amounts to the
same thing, that the pressure in the wake and on the cylinder base is

the free-stream pressure. It is known, however, that the pressure on
the base, behind the separation points, is actually much lower, which
corresponds to a velocity on the free streamline which is higher than
the free-stream value. This lower base pressure accounts for the
higher drag actually observed. Kirchhoff's theory has been applied,
by a long line of successors, to many other cylinder shapes; and indeed
it can be applied in principle to any shape whatever, the difficulty
being only of computation. (In cases such as the circular cylinder,
where there is not a well-defined, fixed separation point, an additional
assumption must be made.) In all cases, however, the theory gives values
of drag much lower than those observed, and always for the reason that
the value assumed for the separation velocity is too low.

Kármán, in his famous theory of the vortex street, attacked the
problem by way of another characteristic feature of flow past bluff
bodies, that is, the phenomenon of periodic vortex shedding. The
theory is incomplete in that it cannot by itself relate the vortex-
street dimensions and velocities to the cylinder dimension and free-
stream velocity. Two additional relations are required, and these must
come from elsewhere, usually from experiment.

These two examples by Kirchhoff and Kármán are, however, represent-
ative of the two parts of the flow that will have to be considered in
any complete theory. While each part - the potential field and the wake -
may be considered separately, the complete solution will only be found by
discovering how to join them. Indeed, Heisenberg (ref. 6) attempted to
obtain such a closed solution by joining the Kirchhoff solution to
Kármán's vortex street. His solution gives a value for the drag in
good agreement with that for a flat plate set normal to the flow, but
it also gives the same value for any other cylinder shape, as pointed
out by Kármán in a footnote to the same paper. There is an inconsis-
tency in the theory in that the Kirchhoff flow, which is taken as one
element in the synthesis, predicts a drag coefficient which is different
(lower) from the final result. In short, the Kirchhoff flow is not a
suitable starting point for such solutions unless it is modified to
allow more realistic base pressures.

In reference 5 it was shown how such a modification may be made.
Instead of restricting the separation velocity to the free-stream
value U_∞, it is allowed to assume an arbitrary value $U_s = kU_\infty$. The
base-pressure coefficient is then $C_{ps} = 1 - k^2$. For $k = 1$ this
reduces to the Kirchhoff case, but for agreement with experiment k
must be greater than 1. This modified Kirchhoff theory will be referred
to as the notched-hodograph theory, after the hodograph upon which it is
based.

Another method by which the potential part of the flow might be
"joined" to the wake is to use the momentum-diffusion theory which has
been applied in calculations of base pressure on supersonic projectiles
(refs. 7 and 8). These calculations are made on the basis of a mixing
theory, wherein the pressure deficiency on the base is assumed to be
"supported" entirely by the diffusion of momentum across the shear layers.
In fact, it appears inevitable that some such calculation will be neces-
sary before a complete theoretical formulation of the problem can be
obtained. The mechanism of the wake immediately downstream of the cylinder
is the main item in the coupling between wake and potential flow, and it
will probably be essential to understand it. Unfortunately, the idea of
simple momentum diffusion across the shear layers, which appears to be
suitable for the supersonic flows, is not by itself sufficient for the
incompressible flow past a bluff cylinder. The "coupling region" imme-
diately downstream of the body is also that in which the vortices are
formed, and they are an essential part of the mechanism, as will be shown
in the following sections.

EFFECT OF VORTEX FORMATION

Figure 1 shows a pressure traverse made along the center line of the
wake behind a flat plate set normal to the flow. The measurement is not
simple to make because of the large transverse velocity fluctuations
associated with the vortex shedding. A static probe oriented along the
center line of the wake experiences a nonstationary crossflow, fluctu-
ating at the shedding frequency. As far as the mean flow is concerned,
the pressure is constant over the circumference of the cylindrical probe,
since its dimensions are small compared with the flow field. Because of
the crossflow, however, there is a pressure variation over the circumfer-
ence, just as there is for a cylinder placed normal to a stream with
periodic velocity. Therefore the pressure measured varies with the
position of the orifice on the circumference of the probe. When the
orifice is at one of the stagnation points of the crossflow the pressure
is the highest, and when it is at 90° from the stagnation point the pres-
sure is the lowest. The pressures measured with the orifice at these
limiting positions are shown in figure 1. The correct pressure should
be somewhere between. Now on a cylinder in steady crossflow the pressure
coefficient is zero at 30° in potential flow and at about 35° in real
flows. It was simply assumed that the latter is also the correct position
for the oscillating crossflow. The intermediate curve in figure 1 is the
result with the orifice at 35° from the stagnation point; it is believed
that this gives very nearly the correct value for the mean static pressure.

In any case, what is important is the low-pressure region at about
2 plate widths downstream; that is, the pressure on the base is not the
lowest pressure in the wake. This measurement had already been made by

Schiller and Linke in 1933 (ref. 9), but does not seem to have been noted since. Its significance seems clear - that the low pressure is associated with a low-pressure region at the center of the vortex which is being formed. This low pressure must fluctuate, of course, as the vortices form alternately, and it is the mean effect which has been measured. It seems likely then that a large part of the low pressure on the base of the flat plate is associated with the vortex pressure, that is, that the main mechanism for the base pressure is to be found not in the diffusion of momentum across the shear layers but in the dynamics of the vortices. In fact, the momentum-diffusion theory could predict only a monotonically increasing pressure from the base.

Now if the vortex dynamics are indeed important, then interference with their formation should have a strong effect on the base pressure. This was easily investigated by placing a "splitter" plate along the center line of the wake. Figure 2 shows pressure distributions with and without the splitter plate. (The results given in this figure are for a circular cylinder instead of the flat plate.) With the splitter plate the periodic vortex formation is inhibited and the base pressure increases considerably. It is still below free-stream pressure, but whether this residual underpressure can be accounted for by the momentum-diffusion theory is not certain. It is possible that a kind of standing vortex is formed on each side, but this point was not investigated further. In any case, the momentum-diffusion theory is indifferent to the omission or inclusion of a partition along the central streamline. It is clear that without the splitter plate the periodic formation of vortices is an essential part of the base-pressure mechanism.

Figure 3 shows how the splitter plate affects the pressure distribution over the whole cylinder circumference. It shows that interference in the "coupling region" changes the outer potential flow, as well as that in the wake.

EFFECT OF INTERFERENCE ELEMENT ON RELATIONS BETWEEN

BASE PRESSURE AND SHEDDING FREQUENCY

In the experiment of figure 2 the chord of the splitter plate was almost 5 diameters. One immediately asks how the interference changes with changing chord. Accordingly, some measurements were made with a splitter plate whose chord was about 1 diameter. This was found not to inhibit the vortex formation at all, though it does change the shedding frequency slightly. More interesting is the effect of moving this short plate downstream, that is, leaving a gap between it and the cylinder. The effect is to decrease the shedding frequency and to increase the base pressure, as shown in the lower part of figure 4. The shedding frequency becomes a minimum, and the base pressure a maximum, when the trailing edge of the interference element is 3.85 diameters downstream of the cylinder

base. It is clear that such a minimum must be reached, for when the
element is very far downstream of the cylinder its upstream influence
should be negligible. What is remarkable is the abrupt jump that occurs
there, practically to the original value. Qualitatively, it appears that
close to the cylinder the element has a streamlining effect; that is, it
extends the shear layers and forces the vortices to form downstream of
its trailing edge. When it is far downstream, the vortices form on its
upstream side, in the normal position close to the cylinder, and the
element has only a slight effect. There must then be some critical posi-
tion where the flow must choose between one of the two configurations.
It is observed, in fact, that when the interference element is at this
critical position, the flow does jump, intermittently, from one configu-
ration to the other, as shown by the double values measured there.

At $c/d = 1.13$ there is a point that does not fall on the line
drawn for C_{ps}. This was thought to be an error, but further checks and
readjustments indicated that it is real. This point corresponds to the
case where the splitter plate was touching the back of the cylinder;
that is, the gap was completely closed. However, the joint was by no
means pressuretight. It seemed, rather, that some other kind of com-
munication through the gap becomes effective at some finite gap width.
At present, this has not been thoroughly investigated.

Experiments such as these may lead to information useful for under-
standing the mechanics of the vortex formation. An initial step in this
direction has been made by investigating the relationship between the
base pressure and the shedding frequency (see the following section).

BLUFF-BODY SIMILARITY

Although a complete theoretical solution seems remote at present,
there is still the possibility of finding a correlation between differ-
ent bluff bodies, on a semiempirical basis. Such a correlation must be
based on, and must account for, the following qualitative facts, which
are indeed the main features of the flow past bluff cylinders:

(1) The "bluffness" of a cylinder is related to the width of the
wake, compared with the cylinder dimension. It is almost intuitive that
the bluffer body tends to diverge the flow more, to create a wider wake,
and to have larger drag.

(2) The shedding frequency is related to the width of the wake, the
relation being roughly inverse, so that the bluffer bodies have the lower
Strouhal numbers.

(3) For a given cylinder the shedding frequency is related to the
base pressure. Generally, an increase in base pressure is accompanied

by a decrease in shedding frequency. This is well illustrated in the case of figure 4 with the interference element (although there an anomalous behavior is observed for $c/d > 3.85$). Thus, for a given cylinder a decrease in wake width corresponds to an increase in drag, which seems at variance with intuition. However, the decrease in width is associated with an increase in "wake velocities," the net effect being an increased wake energy corresponding to the increased drag.

Figure 5 shows measurements of Strouhal number made on three different cylinder shapes. These were a circular cylinder, a 90° wedge, and a "flat plate" normal to the flow. The shedding frequencies were measured by a hot-wire anemometer placed in the wake. The dimensions of the cylinders used are given in table I. (For the circular cylinder, the curve has been taken from ref. 10). At present, one is concerned only with the higher Reynolds numbers, for which the Strouhal number S is distinctly different for the different cylinders, though approximately constant for each individual one. The figure shows that the circular cylinder, 90° wedge, and flat plate are increasingly bluff, in that order.

Figure 6 is a plot of base-pressure coefficient C_{ps} for the same three cylinder shapes. The base pressure p_s was measured at static orifices on the backs of the cylinders. In the case of the circular cylinder the measurement was made at about 130° from the stagnation point, which is in a region of constant pressure (cf. fig. 3) and is believed to be a more significant point for the base pressure than the one at 180°. Figure 6 shows that the differences in base pressure for the different cylinders are not so marked as are the shedding frequencies and that they cannot be ordered in terms of bluffness. Included in the figure are two cases with wake interference - a circular cylinder and a flat plate - for which the increase in base pressure is quite marked. The interference elements which were used are sketched in table I.

The results of figures 5 and 6 have been corrected for tunnel blockage. The scatter in figure 6 is rather large, for the probable error in the calculation of C_{ps} is inherently large; 1-percent accuracy in measurement of pressure and velocity gives only about 5-percent accuracy in C_{ps}.

Now it is well-known that the wakes of different bluff bodies are similar in structure. In every case the flow separates on the two sides of the cylinder, creating free shear layers which continue for a short distance downstream and then "roll up" into vortices, alternately on either side. The region where this occurs, which extends only a few diameters downstream, was referred to in the section "Review of Theory of Flow Past Bluff Bodies" as the coupling region. Because of the similarity in all bluff-cylinder wakes, one would expect to find a parameter to compare the wakes of different cylinders. The clue is in the shedding frequency, as may be demonstrated by a simple dimensional analysis.

Consider two parallel shear layers (sketch 1) which may be imagined to

$$U_S$$

$$d'$$

$$U_S$$
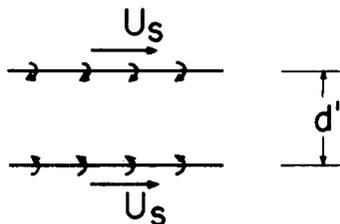
Sketch 1

have been formed by some bluff cylinder. The circular arrows indicate
the sign of the vorticity. The characteristic frequency associated with
this configuration is proportional to U_S/d' and one can define a wake
Strouhal number

$$S* = nd'/U_S$$

where n is the shedding frequency. It is related to the usual cylinder
Strouhal number S by

$$S* = S \frac{U_\infty}{U_S} \frac{d'}{d}$$

$$= \frac{S}{k} \frac{d'}{d} \tag{1}$$

The wake Strouhal number $S*$ is expected to be universal, that is, to be
the same for all bluff-cylinder wakes. Of course this idea is based on
an idealized model in which the shear layers are surfaces of discontinuity,
whereas actually the condition of the free shear layers will differ from
one cylinder to another, depending on their histories up to the point of
vortex formation. This may, however, be a secondary effect, and it is
sufficient at first to assume that $S*$ depends only on a wake Reynolds
number

$$R* = U_S d'/\nu$$

$$= Rk \, d'/d \tag{2}$$

The idea of such a similarity is essentially the same as that given by Fage and Johansen (ref. 3), but they omitted the characteristic wake velocity U_S. Their parameter is $S' = nb'/U_\infty$, where b' is a wake width measured between the outer edges of the shear layers. They found a good correlation, $S' \doteq 0.28$, for several different cylinder shapes, in spite of the omission of a wake velocity. This seems to be due to the fact that, for the cases of good correlation, the wake velocities were very nearly the same. Also, they did not introduce a wake Reynolds number.

In what follows, the wake similarity is studied on the basis of the parameter $S^*(R^*)$. The method, which is quite different from that of Fage and Johansen, depends essentially on the results of the notched-hodograph theory (referred to in the section "Review of Theory of Flow Past Bluff Bodies"). These results are briefly as follows: The velocity at separation and on the initial part of the free streamline is $U_S = kU_\infty$ (sketch 2). The base pressure is the same as that at separation, and the
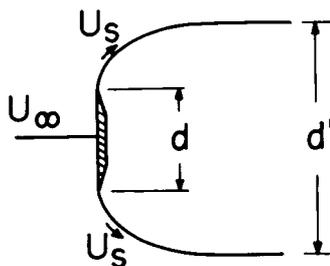
Sketch 2

base-pressure coefficient is therefore $C_{ps} = 1 - k^2$. For a given value of k, the potential flow outside the wake is completely determined, and so the drag coefficient C_D is a function only of k. The important result for the present consideration is that a wake width d' is defined. This also depends only on k. Figure 7, which has been computed from the results of reference 5, shows how d'/d varies with k for the three cylinder shapes being considered. It gives the "measure of bluffness" alluded to earlier; that is, the bluffer cylinders have the wider wakes at a given value of k, but for a given cylinder the wake width decreases with increasing k (i.e., increasing drag).

The shedding frequencies and base pressures which had been measured for figures 5 and 6 were used to compute $S^*(R^*)$ for the various cylinders. The computation is straightforward: $k = \sqrt{1 - C_{ps}}$ is calculated from the measured base-pressure coefficient. The corresponding value of d'/d is found in figure 7. With these and measured values of S and R the corresponding values of S^* and R^* are easily calculated from

equations (1) and (2). The results are listed in table I and plotted in figure 8.

It is necessary to draw attention to several points:

(1) The characteristic wake velocity, which in dimensionless form is simply k, is not measured, but is computed from the base pressure. This may be regarded as the essential step in the coupling between the wake and the outer potential flow.

(2) The wake width is not measured but is obtained from the theory.

(3) In computing S*, the shedding frequency and base pressure should not be first corrected for tunnel blockage. That is, the wake parameters that are used must correspond to the wake that is actually observed. Blockage gives only a second-order effect in this computation. The uncorrected parameters are listed in table I as S_T, R_T, and k_T, respectively.

(4) The errors that may be made in measuring n, U_∞, and $\sqrt{1 - C_{ps}}$, even though small individually (about 1 percent), contribute to a possible error of 4 percent in S*.

(5) At R* < 8,000 there is a large discrepancy between the values for the wedge and for the circular cylinder. It is not clear whether this is real or due to experimental difficulties. The small wedge used to obtain these points did not have a proper base-pressure orifice. Instead, a small tube with an open mouth was cemented to the back of the wedge, and it is not certain that this measures the correct base pressure. Otherwise, the similarity parameter S* does give a good correlation for a fairly wide range of Reynolds number. It is probable that it can be extended to higher Reynolds numbers, say another order of magnitude, up to the critical Reynolds number of the circular cylinder.

It will be noted that the similarity plot (fig. 8) includes the cases with wake interference. For these the base pressure and corresponding wake velocity differ considerably from those without interference. That they fit fairly well into the similarity plot is taken as evidence for the suitability of the parameter S*(R*). Nevertheless, an examination of an individual case shows that there actually is a systematic variation of S*. In the upper part of figure 4 the data of the lower part have been used to calculate S*, which is seen to vary systematically with the position of the interference element. (The "bad point" referred to in the section "Relations Between Base Pressure and Shedding Frequency" does not fit this curve either.)

JOINING THE FREE STREAMLINES AND VORTEX STREET

To close the Kármán theory of the vortex street, two additional relations are needed to relate the velocities and dimensions of the street to the free-stream velocity and cylinder dimension. The notched-hodograph theory may furnish these additional two relations, provided a realistic way can be found to join the results of the two theories.

One relation is obtained by considering how circulation in the vortices is related to the vorticity in the free shear layers. The rate at which circulation flows past any plane section of a shear layer is

$$\int_1^2 \zeta U \, d\eta = \frac{U_1^2 - U_2^2}{2}$$

where ζ is the vorticity and U_1 and U_2 are the velocities at the edges of the shear layer; for the free-streamline case these are $U_s = kU_\infty$ and 0, respectively, and the rate of flow of circulation is $k^2 U_\infty^2/2$. On the other hand, the rate at which circulation is carried downstream by the vortices is $n\Gamma$, where Γ is the circulation per vortex and n is the shedding frequency. The experiments of Fage and Johansen (ref. 3) indicate that only a fraction ϵ of the vorticity in the shear layers is found in the individual vortices farther downstream. They estimated ϵ to be about $1/2$. It is necessary to allow for this in writing the relation between the circulation produced at the cylinder and that carried downstream by the vortices. Thus

$$n\Gamma = \epsilon k^2 U_\infty^2/2$$

or

$$\frac{U_\infty - u}{l} \Gamma = \epsilon k^2 U_\infty^2/2$$

where u is the velocity of the vortices relative to the free stream and l is the spacing along a row. Finally, in dimensionless form,

$$\left(1 - \frac{u}{U_\infty}\right)\frac{\Gamma}{U_\infty l} = \epsilon \frac{k^2}{2} \tag{3}$$

This is similar to the relation obtained by Heisenberg, but he assumed both ϵ and k to be equal to unity.

Equation (3) can be written in another form by introducing one of the Kármán parameters:

$$\frac{\Gamma}{ul} = 2\sqrt{2} \tag{4}$$

Elimination of Γ from equations (3) and (4) gives

$$\frac{u}{U_\infty} = \frac{1}{2}\left(1 \pm \sqrt{1 - \frac{\epsilon k^2}{\sqrt{2}}}\right)$$

which may then be used in Kármán's drag formula

$$C_D = \frac{h}{d}\left[5.65 \frac{u}{U_\infty} - 2.25\left(\frac{u}{U_\infty}\right)^2\right]$$

where h is the width of the vortex street. This is better written in the form

$$C_D \frac{d}{h} = 5.65 \frac{u}{U_\infty} - 2.25\left(\frac{u}{U_\infty}\right)^2 = f(k,\epsilon)$$

On the other hand, from the notched-hodograph theory, one can calculate $C_D(d/d')$ as a function of k, where d' is the distance between the free streamlines. It seems reasonable to assume that $h = d'$, that is,

that the centers of vorticity in the vortex street are the same distance apart as in the free shear layers. This then gives the second relation, simply

$$C_D \, d/h = C_D \, d/d'$$

To find solutions, the left- and right-hand sides are plotted as functions of k. The intersections are the solutions. The left-hand side $C_D(d/h)$ gives a family of curves with ϵ as parameter. The right-hand side gives another family in which the cylinder shape is the parameter. Figure 9 shows the result. The following points should be noted:

(1) The family of curves for different cylinders is actually a single curve (within the width of the line on fig. 9) up to about $k = 1.5$.

(2) There are two possible intersections for each value of ϵ. The upper intersections correspond to $u/U_\infty > 0.5$ and the lower ones, to $u/U_\infty < 0.5$. The latter are the observed values. This empirical fact determines the choice of sign for the square root in the equation for u/U_∞ above.

(3) There are no solutions for ϵ greater than about $1/2$.

To choose the correct value of ϵ, some reference to experiment is necessary; but the circumstance that there is only one curve for all the cylinders reduces the empirical aspect to a minimum, for it is necessary, in principle, to find ϵ experimentally for only one cylinder shape. Another way of expressing this is that the value of k is the same for all cylinders having the same value of ϵ. In fact, it is observed (fig. 6) that the values of k, or of C_{ps}, are approximately the same for the different cylinders (but not when there is interference in the wake). From that figure an average value of k for cylinders without wake interference is 1.4, which gives the solution $C_D(d/d') = 0.96$, $u/U_\infty = 0.18$, and $\epsilon = 0.43$. The corresponding values of the drag coefficient are 1.10, 1.32 and 1.74, for the circular cylinder, 90° wedge, and flat plate, respectively. These may be compared with experimental values: For the circular cylinder C_D varies from about 0.9 to 1.2 in this range of Reynolds number, while for the 90° wedge and flat plate it is about 1.3 and 1.8, respectively, also varying somewhat but less than for the circular cylinder.

The shedding frequencies may also be calculated. In dimensionless terms,

$$S = nd/U_\infty$$

$$= \left(1 - \frac{u}{U_\infty}\right)\frac{d}{l} = \left(1 - \frac{u}{U_\infty}\right)\frac{d}{d'}\frac{h}{l}$$

where again use has been made of the relation $n = (U_\infty - u)/l$ and the assumption $d' = h$. The ratio h/l is the Kármán spacing ratio of 0.281. The universal Strouhal number is then

$$S^* = \frac{0.281}{k}\left(1 - \frac{u}{U_\infty}\right)$$

Using the solution obtained above, this gives $S^* = 0.164$, and for the cylinder Strouhal numbers the values 0.206, 0.167, and 0.127, respectively. These may be compared with the experimental results of figure 5.

DISCUSSION

The similarity parameter $S^*(R^*)$, together with the notched-hodograph theory, reduces to one the number of parameters that must be found empirically in order to have a complete solution. Essentially, it allows the drag to be determined from a measurement of the shedding frequency.[2]

---

[2]To determine the drag for a given cylinder and Reynolds number R, the procedure is as follows: On the $S^*(R^*)$ plot a value of S^* is picked off at a value of R^* which must be guessed, at first, but which may be expected to be a little higher than R. Then the cylinder Strouhal number S is computed from the measured shedding frequency. The ratio $S/S^* = k\, d/d'$ (eq. (1)) essentially gives k from the plot of $k\, d/d'$ versus k (which has not been included here but may easily be obtained from fig. 7). Once k has been determined, the value of $R^* = Rk\, d'/d$ may be computed. If it does not check the original assumed value, then a new value of S^* is found, and the procedure is repeated. No more than the one iteration is necessary, for S^* varies quite slowly with R^*. Once k is determined, the drag is found from the plot of $C_D(k)$ given in reference 5.

The range of Reynolds numbers for which the similarity is valid has not been established. At the upper end similarity will probably exist so long as there is periodic shedding, which for the circular cylinder is up to $R \approx 10^5$. At the lower end it is not certain whether the discrepancy of figure 8 is due only to the experimental difficulty mentioned in the section "Bluff-Body Similarity." More probably, it is insufficient in that range to lump all the Reynolds number effects into the one parameter R^*. An example of the details that may have to be considered is the problem of transition in the free shear layers. At higher Reynolds numbers the layers are turbulent almost from separation, but at lower values they remain laminar for some distance downstream. The point of transition may be expected to be different for different cylinders even at the same R^*, since the shear layers will have experienced different pressure gradients, and so forth. The present solution may be a suitable starting point for a more detailed study of such effects.

The solution obtained by joining the free-streamline flow to the vortex street might also be regarded as a kind of similarity solution, depending on only a single experimental measurement. The Reynolds number dependence does not appear explicitly. Instead, there is a dependence on ϵ, the fraction of the shear-layer vorticity that appears in individual vortices. The interesting result is that for a given ϵ the different cylinders have the same value of k, that is, of base pressure, their drag coefficients then being simply proportional to the wake widths and inversely proportional to the shedding frequencies.

In both cases the need for an additional empirical relation appears to be connected with the need for more understanding of the flow in the region of vortex formation. For this, the technique of wake inteference may prove to be useful.

The results obtained may be applied to cylinder shapes other than the three that were considered so long as they are of comparable "bluffness." For instance, they probably cannot be applied directly to bodies of small percentage thickness, such as a thin wedge, for which the history of the boundary-layer development is quite different from that on bluffer cylinders.

California Institute of Technology,
    Pasadena, Calif., August 13, 1953.

REFERENCES

1. Fluid Motion Panel of the Aeronautical Research Committee and Others
   (S. Goldstein, ed.): Modern Developments in Fluid Dynamics. Vol. II.
   The Clarendon Press (Oxford), 1938.

2. Fage, A., and Johansen, F. C.: On the Flow of Air Behind an Inclined
   Flat Plate of Infinite Span. R. & M. No. 1104, British A.R.C.,
   1927; also Proc. Roy. Soc. (London), ser. A, vol. 116, no. 773,
   Sept. 1, 1927, pp. 170-197.

3. Fage, A., and Johansen, F. C.: The Structure of Vortex Sheets.
   R. & M. No. 1143, British A.R.C., 1927; also Phil. Mag., ser. 7,
   vol. 5, no. 28, Feb. 1928, pp. 417-441.

4. Fage, A.: The Air Flow Around a Circular Cylinder in the Region
   Where the Boundary Layer Separates From the Surface. R. & M.
   No. 1179, British A.R.C., 1928.

5. Roshko, Anatol: A New Hodograph for Free-Streamline Theory. NACA
   TN 3168, 1954.

6. Heisenberg, Werner: Die absoluten Dimensionen der Karmanschen.
   Wirbelbewegung. Phys. Zs., Bd. 23, Sept. 15, 1922, pp. 363-366.
   (Available in English translation as NACA TN 126.)

7. Chapman, Dean R.: An Analysis of Base Pressure at Supersonic Velocities
   and Comparison With Experiment. NACA Rep. 1051, 1951. (Supersedes
   NACA TN 2137.)

8. Crocco, Luigi, and Lees, Lester: A Mixing Theory for the Interaction
   Between Dissipative Flows and Nearly Isentropic Streams. Jour.
   Aero. Sci., vol. 19, no. 10, Oct. 1952, pp. 649-676.

9. Schiller, L., and Linke, W.: Druck- und Reibungswiderstand des
   Zylinders bei Reynoldsschen Zahlen 5000 bis 40000. Z.F.M.,
   Jahrg. 24, Nr. 7, Apr. 13, 1933, pp. 193-198. (Available in English
   translation as NACA TM 715.)

10. Roshko, Anatol: On the Development of Turbulent Wakes From Vortex
    Streets. NACA TN 2913, 1953.

TABLE I

CALCULATED AND MEASURED FLOW PARAMETERS FOR TEST CYLINDERS

Cylinder and symbol (as plotted in figs. 4, 5, 6, and 8)	S_T	R_T	k_T	$\frac{d'}{d}$	S^*	R^*	$\frac{\Delta U_\infty}{U_\infty}$	S	R	k	C_{ps}
A ▫	0.1440	8,030	1.483	1.633	0.159	19,500	0.066	0.135	7,530	1.391	-0.94
	.1411	11,000	1.488	1.625	.154	26,600		.133	10,320	1.396	-.95
	.1428	12,130	1.462	1.674	.162	29,700		.133	11,400	1.372	-.88
2.46 cm	.1449	13,640	1.460	1.680	.167	33,500		.136	12,800	1.370	-.88
	.1441	15,950	1.458	1.682	.166	39,100		.135	14,960	1.368	-.87
	.1442	17,900	1.445	1.710	.171	44,200		.135	16,800	1.356	-.84
	.1410	3,220	1.427	1.742	.173	8,030		.133	3,020	1.339	-.80
	.1490	3,900	1.450	1.700	.175	9,610		.140	3,680	1.360	-.85
.23	.1420	4,190	1.428	1.747	.174	10,440		.133	3,930	1.340	-.80
	.1440	5,670	1.470	1.659	.162	13,800		.135	5,320	1.380	-.90
	.1410	6,320	1.450	1.700	.166	15,600		.132	5,930	1.360	-.85
	.1420	6,610	1.427	1.742	.174	16,500		.133	6,200	1.339	-.80
B ▪	.1420	7,950	1.456	1.682	.164	19,500		.133	7,450	1.366	-.88
	.1430	3,850	1.456	1.700	.168	9,500	.044	.137	3,690	1.392	-.93
1.48	.1425	4,790	1.455	1.690	.165	11,800		.136	4,590	1.391	-.94
	.1418	5,860	1.462	1.678	.163	14,400		.136	5,610	1.400	-.95
	.1407	7,060	1.447	1.706	.166	17,400		.135	6,760	1.383	-.91
.24	.1401	7,900	1.453	1.700	.164	19,500		.134	7,570	1.390	-.93
	.1401	8,860	1.462	1.675	.161	21,700		.135	8,500	1.400	-.96
	.1410	9,630	1.441	1.721	.169	23,900		.135	9,220	1.380	-.90
	.1408	10,630						.135	10,200		
ᵃC ◣	.1408	11,110	1.448	1.705	.166	27,400		.135	10,600	1.385	-.92
.160											
.080											
D ○	.2060	5,850	1.334	1.206	.186	9,400	.020	.202	5,730	1.309	-.71
	.2065	7,150	1.368	1.151	.174	11,250		.203	7,000	1.340	-.80
	.2067	9,920	1.389	1.128	.168	15,500		.205	9,720	1.360	-.85
	.2041	11,650	1.397	1.120	.164	18,200		.200	11,400	1.370	-.88
d=2.22 cm	.2010	13,200	1.400	1.116	.160	20,600		.197	12,900	1.372	-.88
	.2015	14,200	1.401	1.114	.160	22,200		.198	13,900	1.375	-.89
	.2004	17,130	1.421	1.093	.154	26,700		.197	16,800	1.394	-.94
	.2020	15,220	1.420	1.096	.156	25,800		.198	14,900	1.392	-.94
	.2100	885	1.395	1.120	.169	1,380	.004	.209	880	1.390	-.93
	.2110	956	1.380	1.148	.176	1,510		.210	950	1.375	-.89
	.2097	1,078	1.350	1.179	.183	1,720		.209	1,070	1.345	-.81
	.2097	1,270	1.329	1.215	.192	2,050		.209	1,265	1.324	-.75
E	.2124	1,510	1.342	1.190	.188	2,420		.212	1,500	1.337	-.79
	.2075	1,700	1.322	1.230	.193	2,770		.207	1,690	1.317	-.74
	.2065	1,935	1.311	1.250	.197	3,180		.206	1,930	1.306	-.71
d=0.638	.2088	2,145	1.322	1.230	.194	3,500		.208	2,135	1.317	-.74
	.2103	2,950	1.322	1.230	.196	4,800		.210	2,940	1.317	-.74
	.2090	3,250	1.339	1.205	.188	5,250		.208	3,240	1.334	-.78
	.2091	3,675	1.330	1.243	.195	6,060		.208	3,660	1.325	-.76
	.2090	3,950	1.340	1.195	.186	6,330		.208	3,930	1.335	-.78
	.2081	4,330	1.338	1.200	.187	6,950		.207	4,310	1.333	-.78
	.2050	4,890	1.340	1.195	.183	7,810		.204	4,870	1.335	-.78
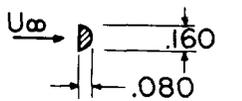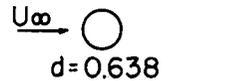
ᵃNo base-pressure measurements made.

TABLE I.- Concluded

CALCULATED AND MEASURED FLOW PARAMETERS FOR TEST CYLINDERS

Cylinder and symbol (as plotted in figs. 4, 5, 6, and 8)	S_T	R_T	k_T	$\frac{d'}{d}$	S*	R*	$\frac{\Delta U_\infty}{U_\infty}$	S	R	k	C_{ps}
F (△, 90°, 3.10)	0.1886	4,160	1.473	1.315	0.168	8,060	0.054	0.179	3,940	1.395	-0.95
	.1910	5,050	1.515	1.291	.163	9,880		.181	4,790	1.437	-1.07
	.1831	7,130	1.497	1.300	.159	13,900		.174	6,750	1.419	-1.01
	.1845	8,150	1.482	1.310	.163	15,800		.175	7,730	1.404	-.97
	.1878	8,750	1.497	1.300	.163	17,000		.178	8,300	1.419	-1.01
	.1881	10,400	1.492	1.303	.164	20,200		.178	9,850	1.414	-1.00
	.1841	12,930	1.482	1.310	.163	25,100		.175	12,300	1.404	-.97
	.1883	15,270	1.497	1.300	.164	29,700		.179	14,500	1.419	-1.01
	.1882	16,920	1.485	1.308	.166	32,900		.178	16,000	1.407	-.98
	.1854	19,110	1.480	1.311	.164	37,100		.176	18,100	1.402	-.97
	.1905	7,180	1.489	1.306	.167	13,900		.181	6,800	1.411	-.99
	.1856	8,430	1.480	1.311	.165	16,400		.176	7,980	1.402	-.97
	.1849	9,400	1.495	1.302	.161	18,300		.175	8,900	1.417	-1.01
	.1846	11,040	1.487	1.305	.162	21,400		.175	10,500	1.409	-.99
	.1855	13,660	1.499	1.300	.161	26,600		.176	12,900	1.421	-1.02
	.1880	15,320	1.497	1.300	.163	29,900		.178	14,500	1.419	-1.01
	.1852	17,300	1.490	1.304	.162	33,600		.176	16,400	1.412	-.99
	.1848	19,210	1.478	1.312	.164	37,200		.175	18,200	1.400	-.96
	.1866	20,600	1.490	1.304	.163	40,000		.177	19,500	1.412	-.99
	.1872	22,700	1.489	1.306	.164	44,000		.177	21,500	1.411	-.99
G (▲, .430 cm)											
H (△, .430, .08 Pressure tube)	.1826	1,210	1.461	1.322	.165	2,340	.010	.181	1,200	1.446	-1.09
	.1830	1,380	1.457	1.326	.167	2,665		.181	1,370	1.442	-1.08
	.1865	1,570	1.480	1.310	.165	3,040		.185	1,550	1.465	-1.15
	.1845	2,030	1.476	1.312	.164	3,930		.183	2,010	1.461	-1.14
	.1832	2,240	1.495	1.301	.160	4,350		.181	2,220	1.480	-1.19
	.1824	2,510	1.483	1.310	.161	4,870		.181	2,490	1.468	-1.16
	.1820	2,750	1.488	1.306	.160	5,330		.180	2,722	1.473	-1.17
	.1818	3,030	1.488	1.306	.160	5,880		.180	3,000	1.473	-1.17
	.1846	3,400	1.492	1.303	.161	6,610		.183	3,370	1.477	-1.18
J (▱, 2.46 cm, 2.54, 10)	.0998	5,600	1.311	2.115	.161	15,600	.066	.094	5,250	1.230	-.51
	.1008	6,430	1.301	2.162	.167	18,000		.095	6,030	1.220	-.49
	.1002	6,750	1.323	2.063	.156	18,400		.094	6,340	1.241	-.54
	.1030	7,650	1.303	2.155	.170	21,300		.097	7,180	1.223	-.50
	.1006	6,950	1.342	1.990	.149	18,600		.094	6,500	1.260	-.59
	.1036	8,360	1.330	2.035	.159	22,600		.097	7,850	1.248	-.56
	.1071	11,110	1.350	1.963	.156	29,500		.101	10,400	1.266	-.60
	.1060	12,650	1.330	2.035	.162	34,200		.099	11,900	1.248	-.56
	.1049	14,150	1.330	2.035	.161	38,200		.098	13,300	1.248	-.56
	.1048	15,930	1.330	2.035	.160	43,100		.098	15,000	1.248	-.56
	.1041	17,820	1.323	2.060	.162	48,500		.098	16,700	1.241	-.54
K (○, 2.54, 2.22, 6)	.1500	5,960	1.268	1.370	.162	10,350	.020	.147	5,850	1.242	-.54
	.1459	7,370	1.270	1.351	.155	12,700		.143	7,220	1.245	-.55
	.1396	10,230	1.258	1.385	.154	17,900		.137	10,100	1.232	-.52
	.1381	11,400	1.240	1.445	.161	20,400		.135	11,200	1.216	-.48
	.1374	12,860	1.244	1.430	.158	22,900		.135	12,600	1.221	-.49
	.1367	14,100	1.236	1.461	.162	25,500		.134	13,800	1.211	-.47
	.1371	15,600	1.246	1.425	.157	27,700		.135	15,300	1.220	-.49
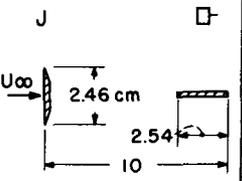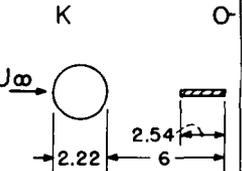
[a]No base-pressure measurements made.
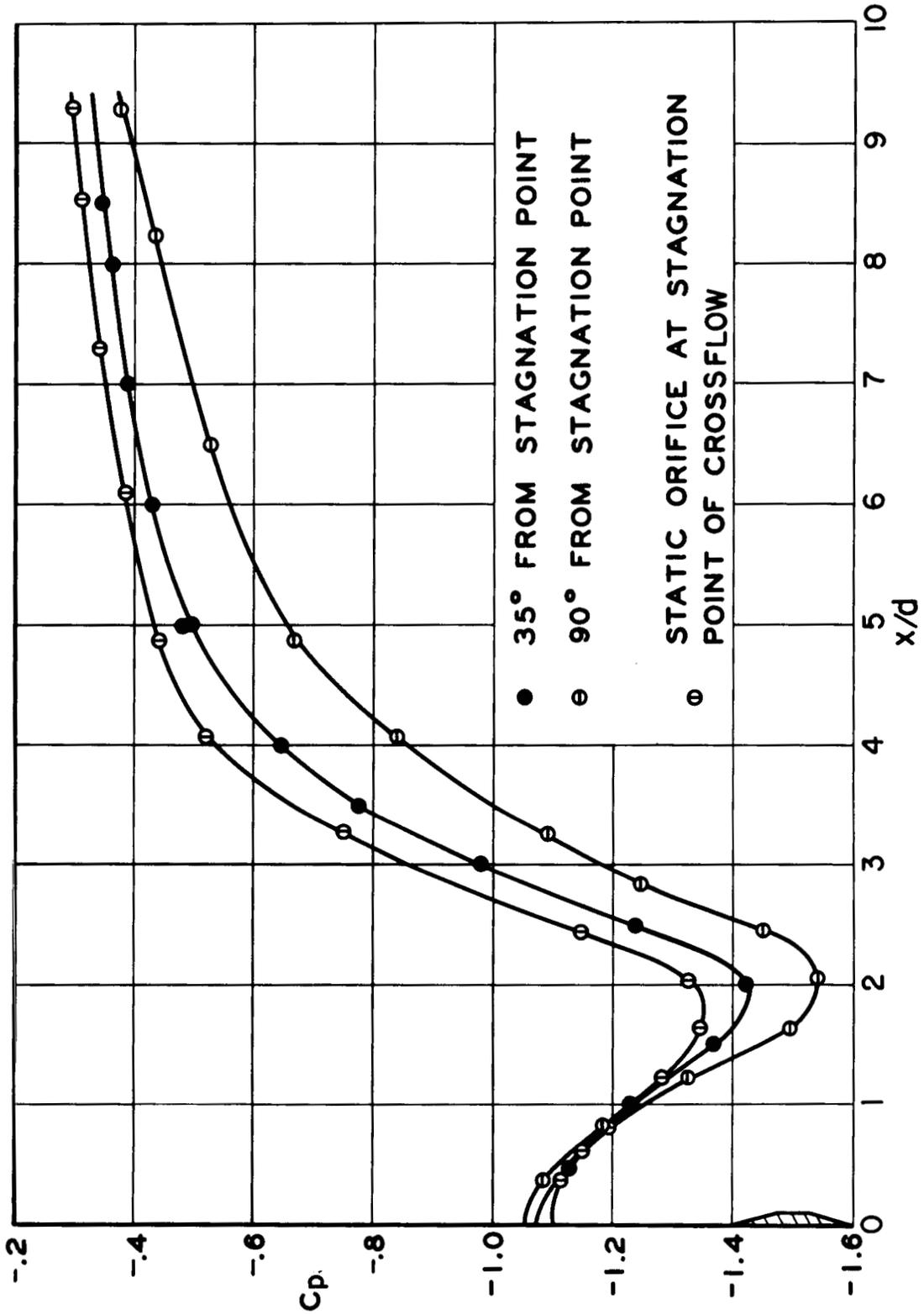
Figure 1.- Pressure on wake center line. R = 14,500.
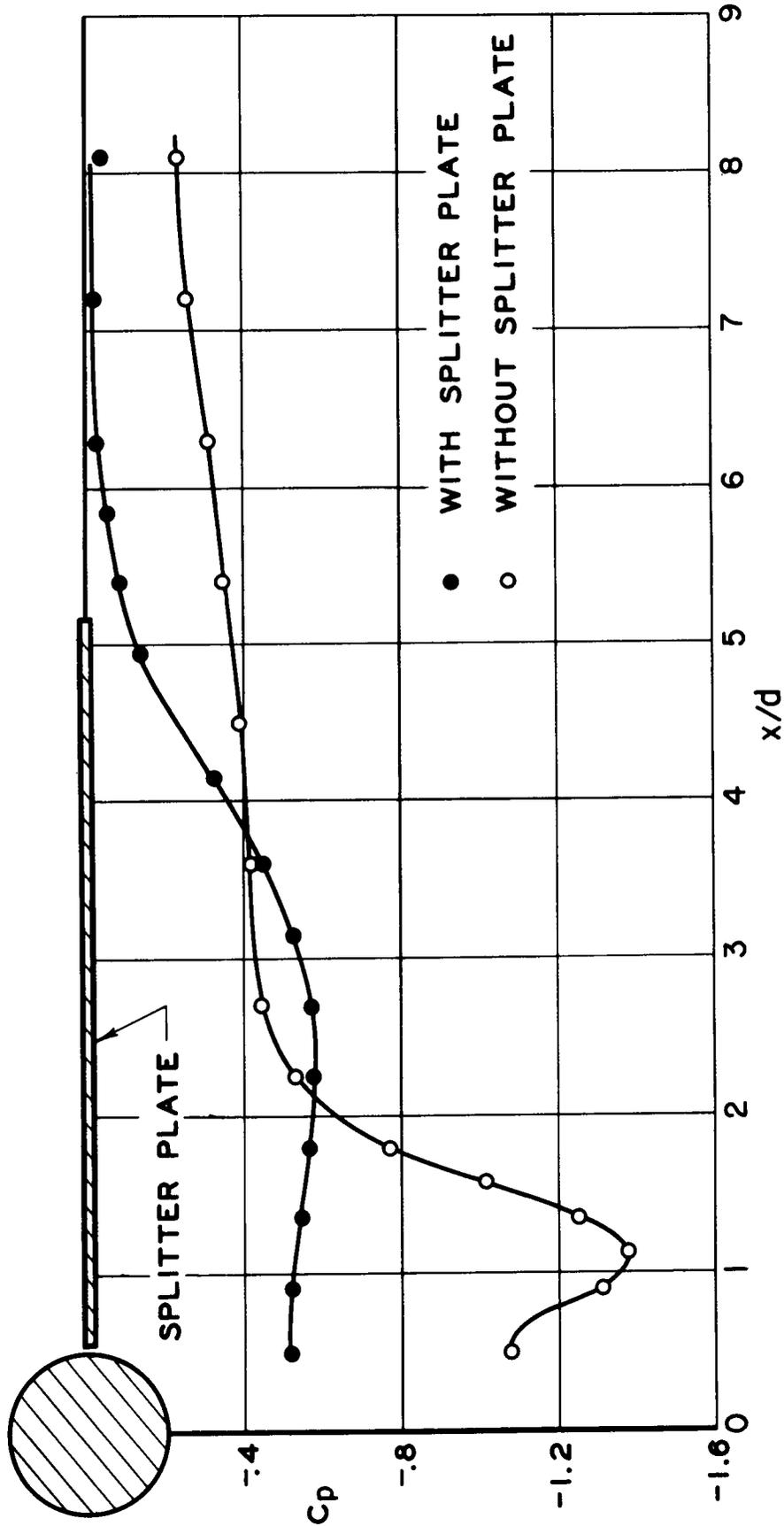
Figure 2.- Pressure on wake center line with and without splitter plate.
R = 14,500.
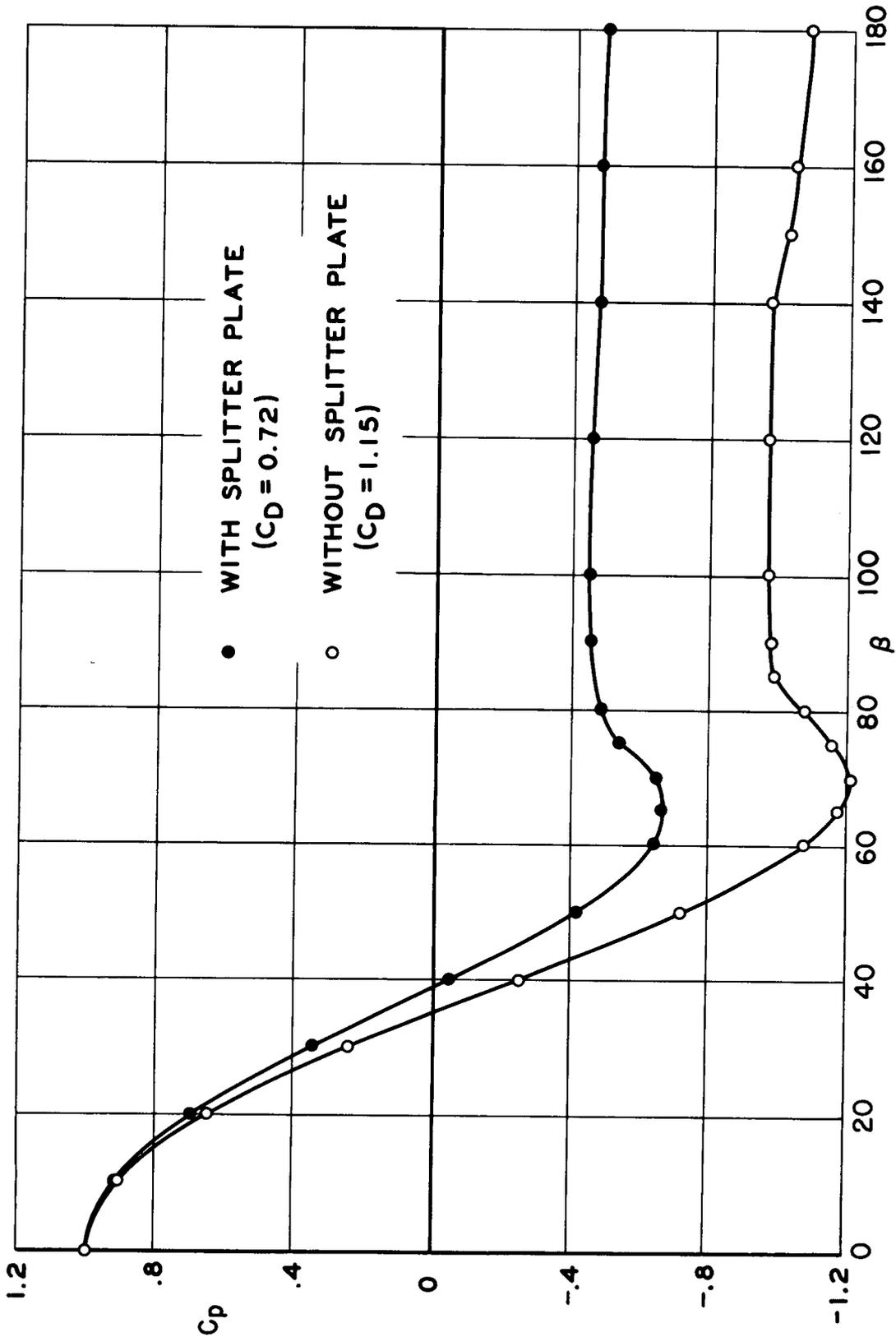
Figure 3.- Pressure on cylinder. R = 14,500.
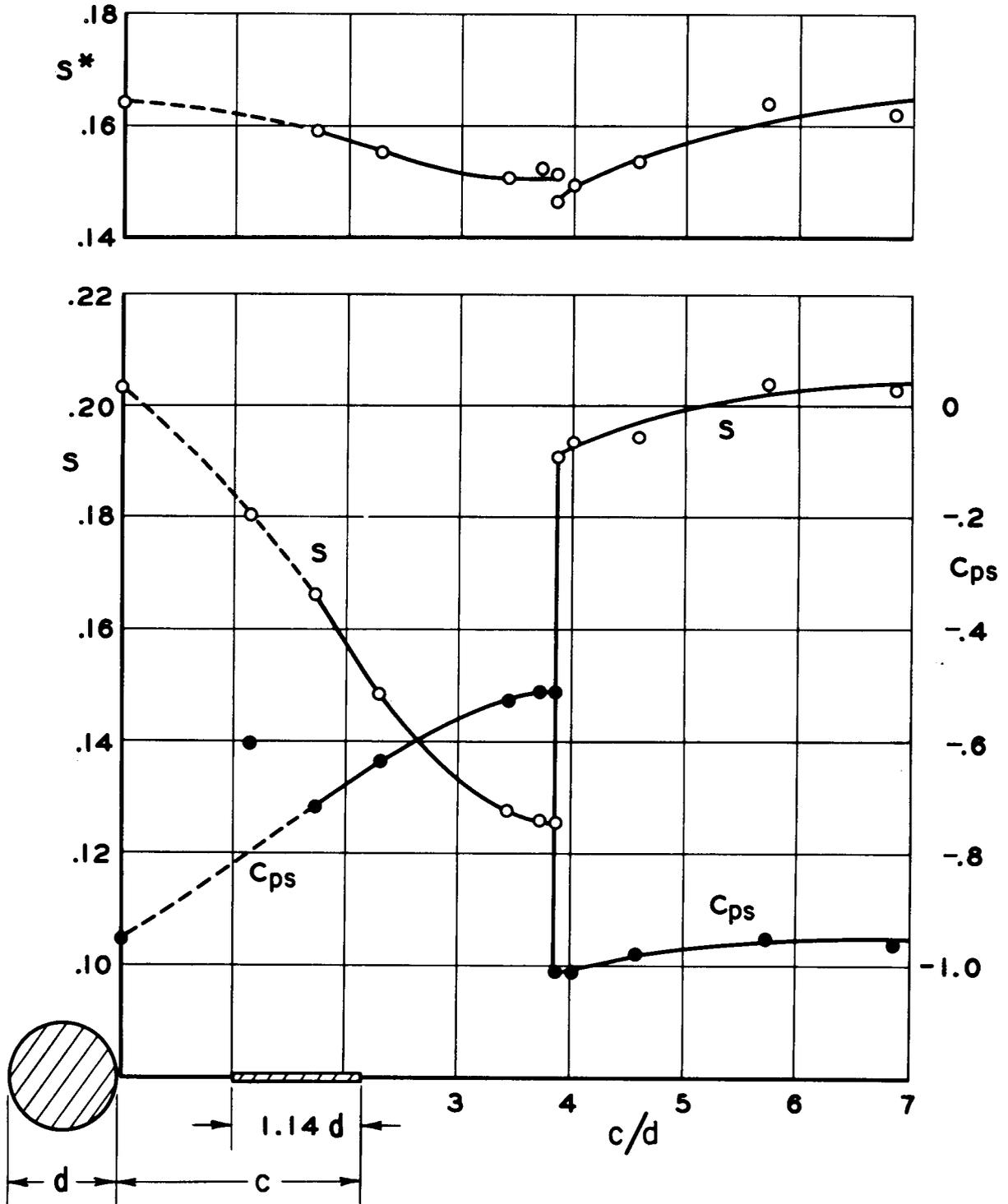
Figure 4.- Wake interference.
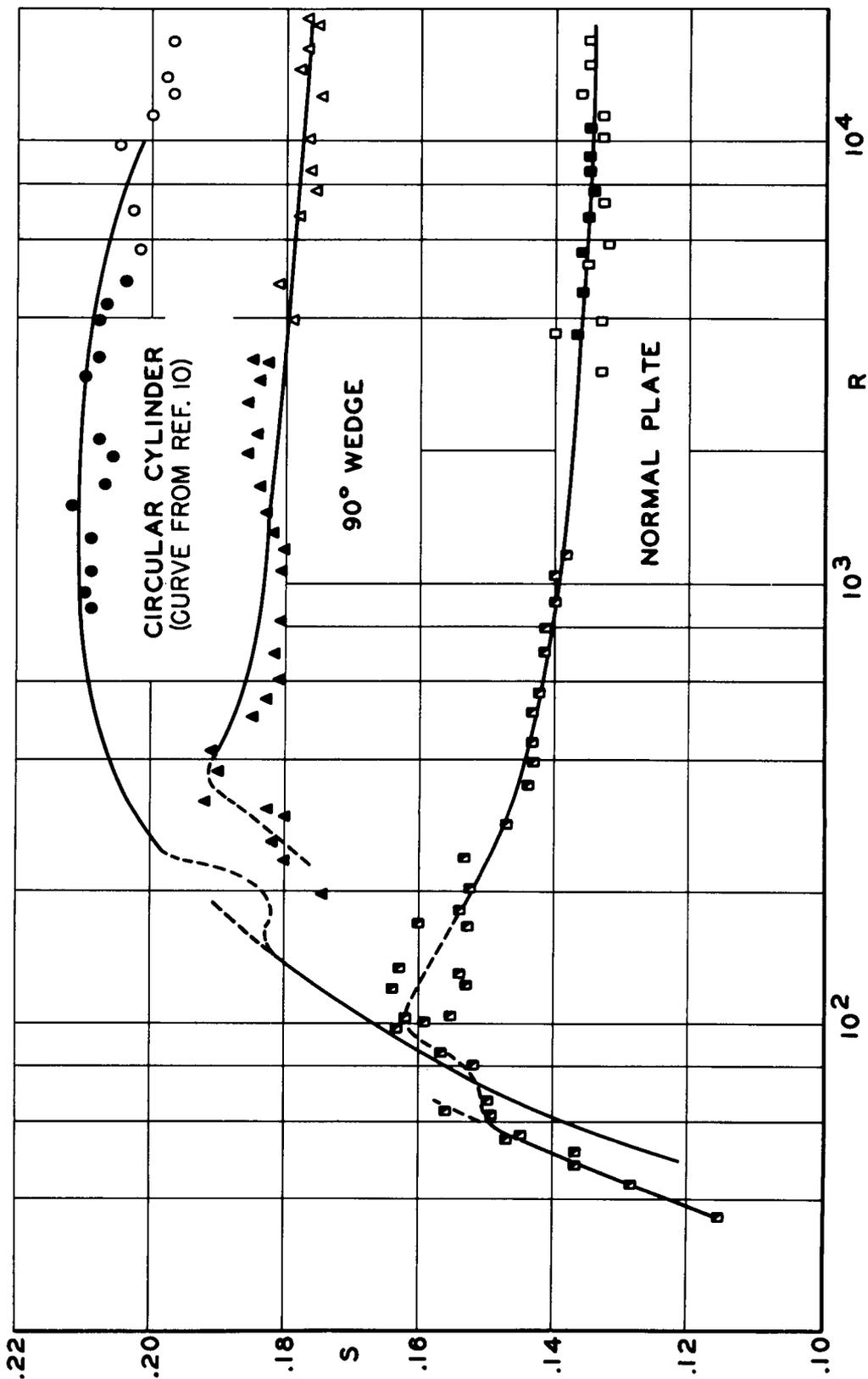
Figure 5.- Cylinder Strouhal number.
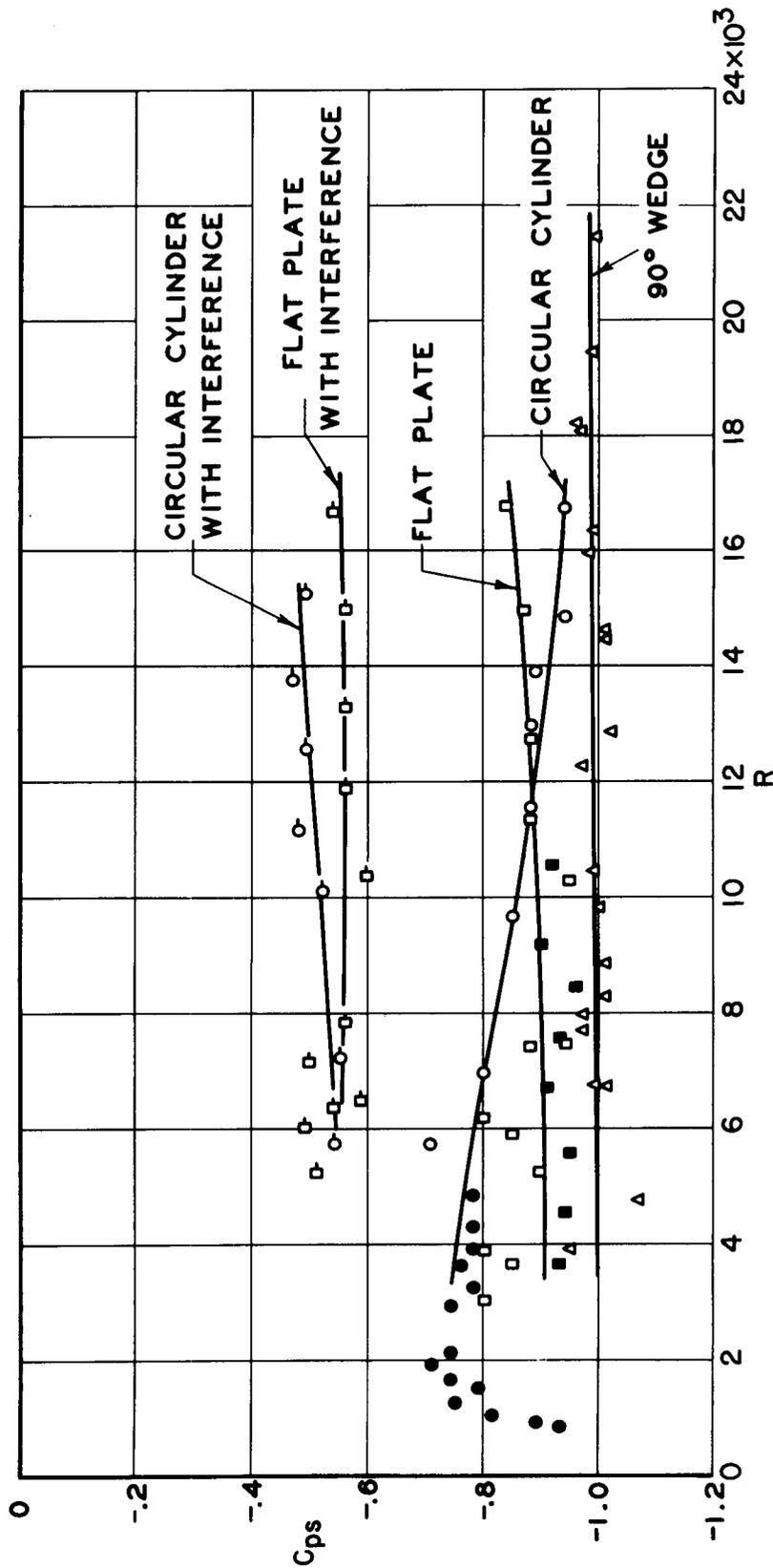
Figure 6.- Base-pressure coefficients.
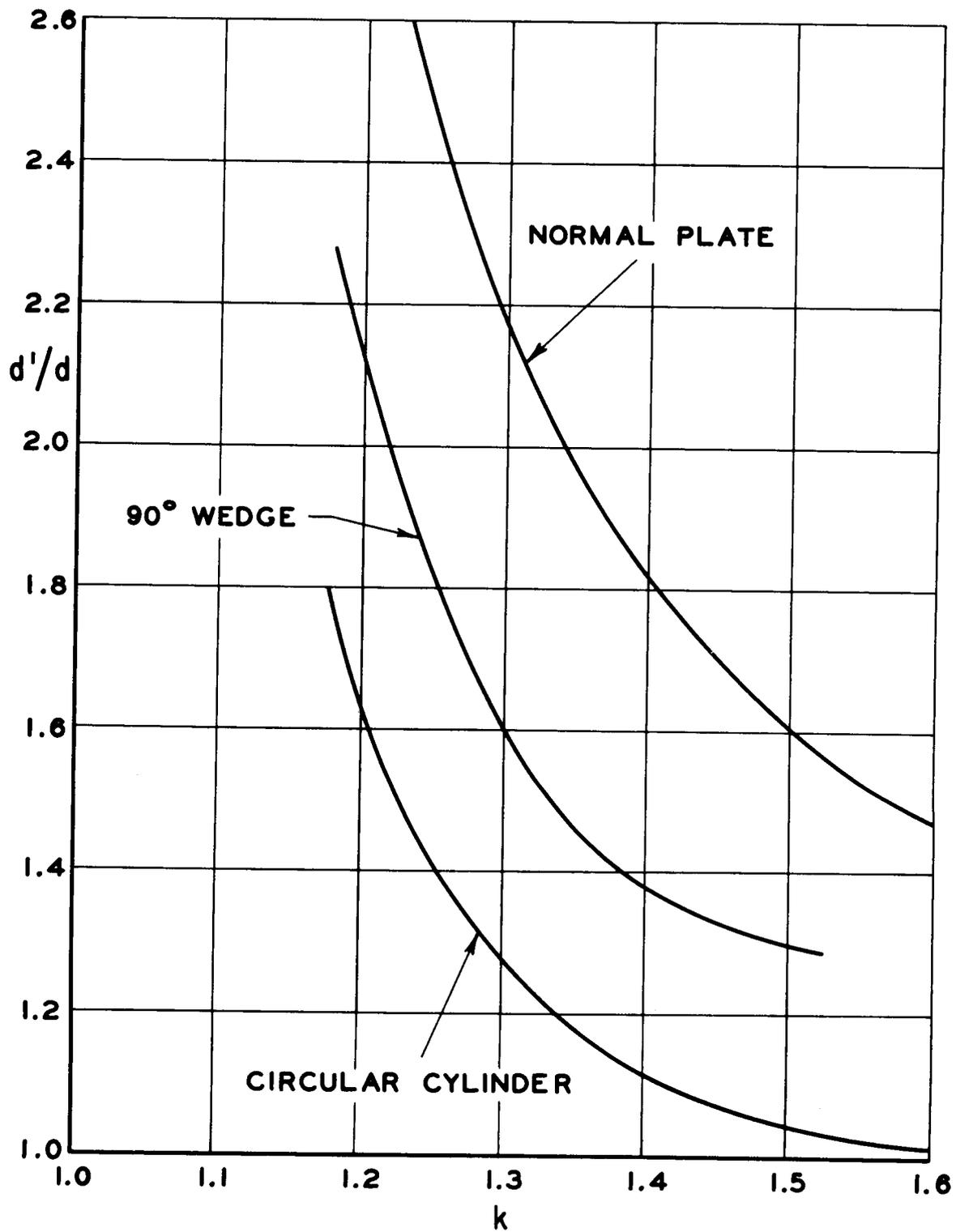
Figure 7.- Wake width.

Figure 8.- Wake Strouhal number.

Figure 9.- Wake solutions.